

# POLYMER MEMS SYSTEM FOR MEASURING THE MECHANICAL MODULUS OF A BIOLOGICAL CELL

Wenyue Zhang<sup>1</sup>, Markus Gnerlich<sup>1</sup>, Yaohua Sun<sup>1</sup>, Gaoshan Jing<sup>1</sup>, Jonathan J. Paly<sup>2</sup>  
Arkady Voloshin<sup>2,3</sup> and Svetlana Tatic-Lucic<sup>\*1,2</sup>

<sup>1</sup>*Sherman Fairchild Center, Electrical & Computer Engineering Department*

<sup>2</sup>*Bioengineering Program*

<sup>3</sup>*Department of Mechanical Engineering & Mechanics, Lehigh University, Bethlehem, Pennsylvania 18015, USA*

*\* svt2@lehigh.edu*

Keywords: Cell mechanics, mechanical modulus, MEMS, polymer, dielectrophoresis.

Abstract: The measurements of the mechanical modulus of biological cells are critical to studies of pathophysiology and the research for an effective treatment. This research has developed a rapid and cost effective technique in order to measure the Poisson's ratio and mechanical modulus of a live biological cell by utilizing microelectromechanical system (MEMS) techniques in a biological application. The design, fabrication, and characterization of a polymer-based MEMS system that integrates a V-shaped electrothermal actuator array and a cell-positioning system in a single microelectronics chip are presented here. This BioMEMS device compressed a NIH3T3 fibroblasts cell and caused up to 25% mechanical strain.

## 1 INTRODUCTION

Osteoporosis is a public health problem that affected more than 44 million Americans in 2004, most of them are women and/or seniors (U.S. Department of Health and Human Services, 2007). This age-related disease results in bones that lack the ability to respond to dynamic mechanical stimulus, which is required for the bones in the human musculoskeletal system to maintain proper osteogenesis (Fritton, McLeod, and Rubin, 2000). Since several properties of bone cells, such as adaptation (Caillot-Augusseau, Lafage-Reoust, Soler, Pernod, Dubois, and Alexander, 1998) and the cytosolic calcium response to fluid flow (Donahue, Zhou, Li, and McCauley, 1997), have been proven to decrease as a function of age, biologists hypothesize that the biomechanical properties of osteoblasts (bone-formation cells) change as a function of age, and this change could be a contributing factor to the pathogenesis of osteoporosis (You, Yellowley, Donahue, Jacobs, 1999).

However, this hypothesis has not been carefully examined due to the limitations of current measurement techniques, such as atomic force microscopy (AFM), which tests the mechanical properties of one small portion of the cell, and can only test one cell at a time. Testing cells one-by-one

is too time-consuming and expensive to be commonly practiced in biological research, which relies on statistical studies that require surveying a large number of cells. As a result, the mechanism underlying the pathophysiology of osteoporosis is still unknown.

To improve the public health condition, it is absolutely necessary to develop efficient techniques to measure cell's mechanical properties. Recently, several MEMS devices have been applied to biological researches, such as a MEMS-based force sensor (Yang and Saif, 2006), and a frequency dependent electrostatic actuator (Scuor, Gallina, Panchawagh, Mahajan, and Sbaizero, 2006). Compared to these single crystal silicon and polysilicon devices, polymer devices have several advantages, such as: less possibility of damaging live cells when making physical contact due to the low Young's modulus of polymers; lower cost (Elderstig and Larsson, 1997); and lastly, the ability to operate in liquids if an electrothermal actuation mechanism is used (the heat is insulated due to the low thermal conductance of polymers). This paper reports a polymer-based MEMS system for measuring the mechanical properties of a live cell.

## 2 METHODOLOGY

To measure the mechanical modulus of a biological cell, a BioMEMS device was designed and fabricated (Figure 1). In a  $2.2 \times 2.5 \text{ mm}^2$  single chip, a polymer electrothermal actuator (ETA) array (1) is to compress a live cell against a fixed wall (2), and report associated forces and displacements during the compression. In addition, a cell positioning system (dielectrophoresis quadrupole electrodes (3)) is used to trap a cell at a desired location, and a set of scale bars (4) is used to calibrate the optical measuring system.

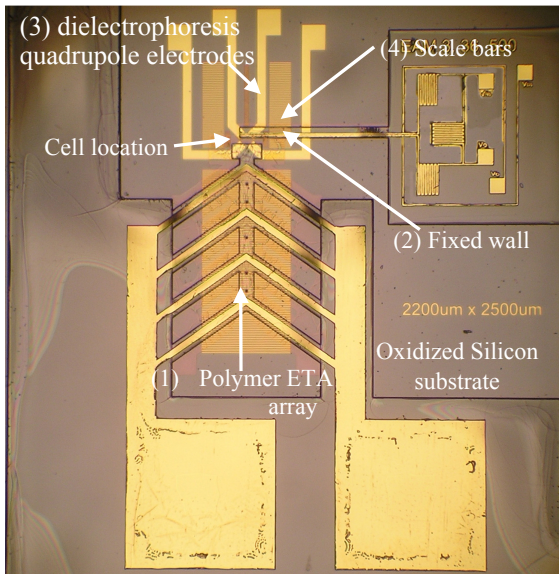


Figure 1: Optical image of a fabricated BioMEMS device for measuring the mechanical modulus of a biological cell.

Four experimental steps need to be done before obtaining the mechanical properties of a cell: (a) characterizing the actuator displacement as a function of input electrical power; (b) determining the reaction force between the actuator and the cell; (c) recording the force versus deformation curve for the cell; (d) fitting the curve with equation (1), which which was based on the derived Hertz contact model (Timoshenko and Goodier, 1970):

$$F = \left( \frac{2\sqrt{2dE}}{3\pi(1-\nu^2)} \right) \Delta d^{\frac{3}{2}} \quad (1)$$

where  $F$  was the applied force to a cell,  $\Delta d$  was cell deformation,  $E$  was compressive modulus of the cell,  $d$  was the diameter of a cell, and  $\nu$  was the Poisson's ratio of the cell. The fitted parameter reveals the mechanical modulus of the cell.

## 3 MEMS DEVICE FABRICATION

Fabrication of the MEMS devices utilized surface micromachining techniques. The processing flow has been described in detail previously (Zhang, 2007), and will be briefly summarized here (Figure 2). The starting materials are oxidized 3-inch diameter silicon wafers. First, a metal layer of 80 nm platinum was patterned using lift-off process (Figure 2a). A 20 nm titanium layer preceding this conductive layer was used to increase the adhesion wherever metallization was present. Second, a 5  $\mu\text{m}$  thick sacrificial photoresist (AZ P4620, Clariant, New Jersey) was applied to create an air gap (Figure 2b). Third, a thick negative tone photoresist (SU-8, product #: 2015, Microchem, MA) was used for a structural layer (Figure 2c). Next, the second metal layer of 80 nm gold (with the same adhesion layer) was patterned on top of the structural polymer (Figure 2d). Finally, the whole structure was immersed in AZ 400T photoresist stripper (Clariant, New Jersey) at room temperature to release the polymer device (Figure 2e).

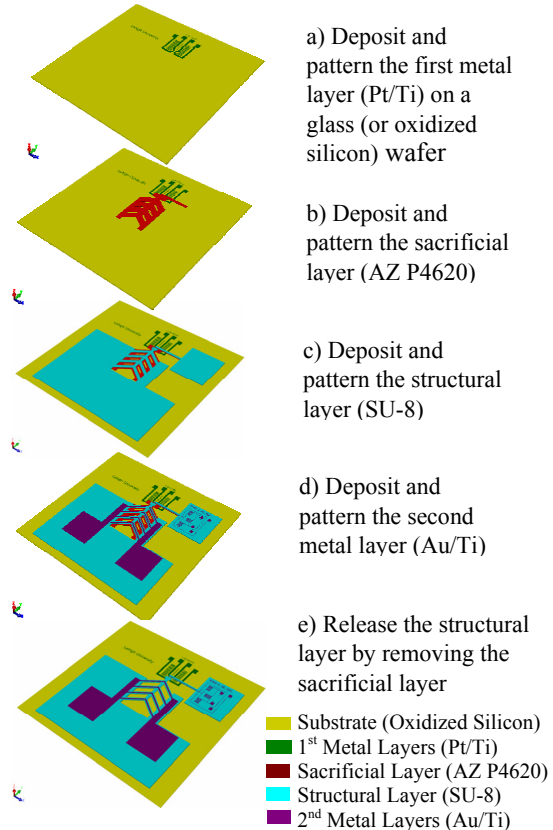


Figure 2: Fabrication process flow for the BioMEMS device for measuring the mechanical modulus of a biological cell.

### 3.1 Effects of UV/Ozone Treatment

A UV/Ozone cleaner was used to clean the substrates and harden the sacrificial pattern (AZ P4620). Without this step, the sacrificial pattern was destroyed during the spin-coating of the structural SU-8 polymer (Figure 3) by centrifugal forces and/or solvent diffusion. During the UV/Ozone treatment, the deep UV light (in ranges of 185 nm to 254 nm wavelength) hardened the thick sacrificial photoresist (Allen, Foster, and Yen, 1982) while the heat generated by the UV lamps added additional cross-linking. Therefore, the sacrificial patterns can maintain their shapes after SU-8 patterning. We used polymer sacrificial materials because it was too difficult to selectively remove a metal sacrificial layer with the pre-patterned Pt/Ti layer on the substrate.

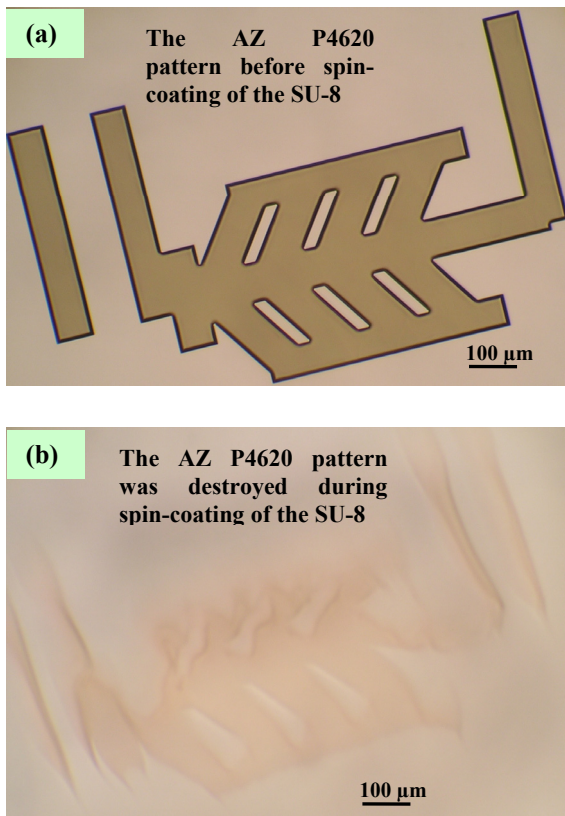


Figure 3: Optical images of the sacrificial patterns (a) before and (b) after spin-coating a transparent structural layer. These sacrificial patterns did not have UV/Ozone treatment and were destroyed.

One more benefit of an UV/Ozone treatment was reduction of gas bubbles in the resist. During the UV exposure of SU-8, the underlying AZ P4620 that had not been previously exposed also absorbed UV

radiation. Then, gases due to photoresist outgassing in UV light (Kunz, 2004) were trapped by the SU-8 layer, which causes gas bubbles formation (Figure 4).

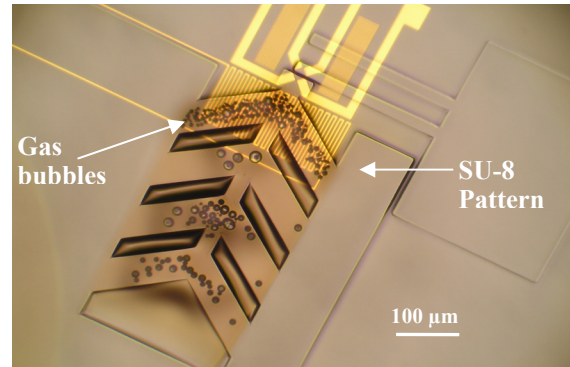


Figure 4: Optical image of gas bubbles that appeared the post exposure baking after UV exposure of the structural layer (SU-8).

Short UV/Ozone treatment (3 to 4 minutes) was applied to solve the gas bubbles problem and resulted in a sacrificial pattern hard enough to resist physical and chemical damage (Figure 5), but still able to be removed at the end of processing.

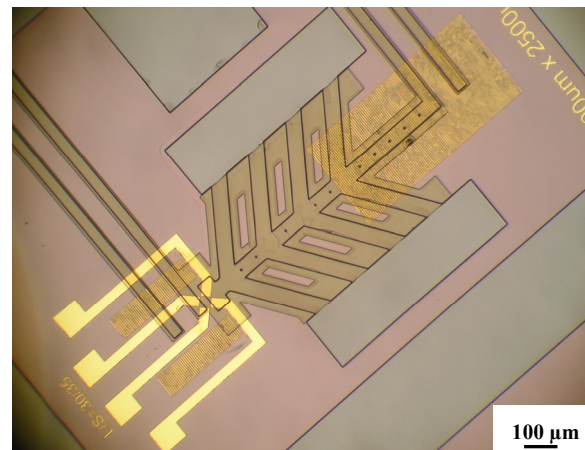


Figure 5: Optical image of a fabricated device. After selecting the proper UV/Ozone treatment time, the sacrificial patterns keep their shapes after SU-8 patterning. (This image was taken after developing the SU-8 layer but before the second metal layer formation).

## 4 RESULT & DISCUSSION

High frequency (800 KHz, sinusoidal) AC voltages were applied to these BioMEMS devices to avoid electrolysis, which generates a large amount of gas in liquids (Selvaganapathy, Leung Ki, Renaud, and



Mastrangelo, 2002). The actuator displacement as a function of input electrical power was recorded (Figure 6) when operation in NIH3T3 fibroblasts cell medium. The maximum displacement was  $4 \mu\text{m}$  when power was RMS 750 mW. After exceeding the maximum value, the displacement decreased due to the out-of-plane deformation of the polymer V-shaped electrothermal actuator array.

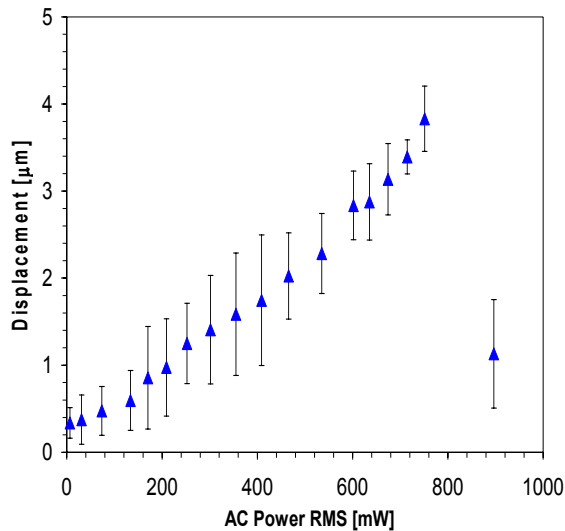


Figure 6: Experimental data of the BioMEMS ETA arrays' displacement as a function of input AC power.

The lab experiments started with immersion of the BioMEMS device into the cell medium. Cells were transferred to the device using a micropipette. First, a cell was trapped at the centre of the dielectrophoretic quadrupole electrodes after applying an AC voltage ( $10 \text{ V}_{\text{p-p}}$ , 1 MHz, sinusoidal) to them (Figure 7a). Next, the actuator was moved towards the cell, and it compressed the cell up to  $4 \mu\text{m}$  (Figure 7b). The diameter of the cell under test was measured to be  $16 \mu\text{m}$ . This means that the BioMEMS devices can mechanically stimulate the cell in 25% strain, which is double the minimum requirement (10% strain) of mechanical stimulation to a cell (You, Cowin, Schaffler, and Weinbaum, 2001).

When the cell was under compression, orthogonal extension was observed as well. Currently, the displacement resolution was  $\pm 0.5 \mu\text{m}$ . Next, the spring constant of the polymer ETA was calibrated using a nanoindenter (TriboScope, Hysitron Inc.). Finally, the compressive modulus of the NIH3T3 fibroblast cell can be extracted from these measurements. In order to extract reliable mechanical modulus, we are currently working on improving the resolution of this method.

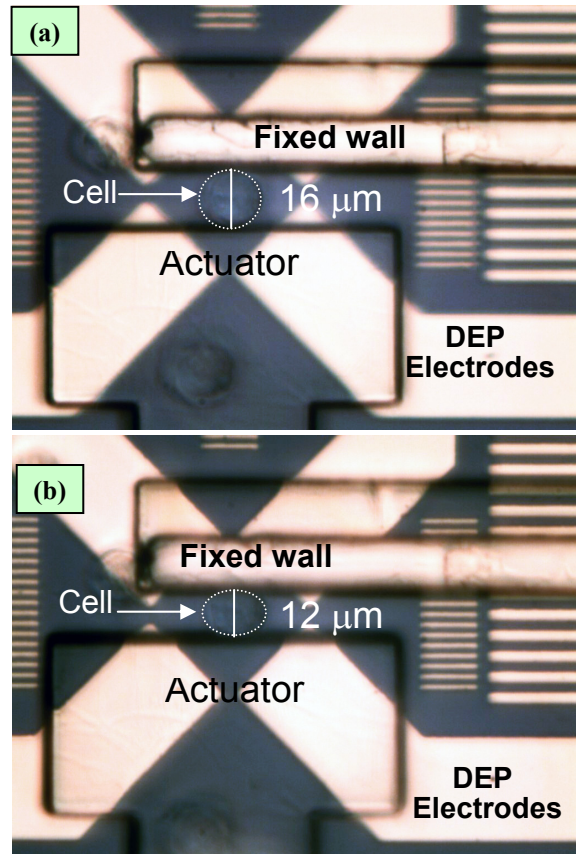


Figure 7: Optical images of: (a) a cell being trapped at the centre of dielectrophoretic quadrupole electrodes, and (b) the cell being compressed by the actuator after being powered up. (Outline of the cell is for better visibility).

## 5 CONCLUSIONS

The measurements of the mechanical properties of biological cells are critical to improve the public health condition. This research focuses on the design, fabrication, and characterization of a MEMS system to measure the compressive modulus of a live biological cell. This MEMS-based system has realized three basic functions: (1) trapping a cell to a designed area before testing; (2) applying forces to a cell, and (3) sensing the forces and displacements during the compressing. The device was able to compress a cell up to 25% mechanical strain in a cell medium. The measurements of mechanical properties are limited by the current displacement resolution and the improvements are under investigation.

## REFERENCES

- Allen, R., Foster, M., Yen, Y.-T., 1982. Deep U.V. Hardening of positive photoresist patterns. *J Electrochem. Soc.*, 128, 1379.
- Caillot-Augusseau, A., Lafage-Reoust, M.-H., Soler, C., Pernod, J., Dubois, F., Alexander, C., 1998. Bone formation and resorption biological markers in cosmonauts during and after a 180-day space flight (Euromir 95). *Clin. Chem.* 44(3), 578-585.
- Donahue, H. J., Zhou, Z., Li, Z., McCauley, L. K., 1997. Age-related decreases in stimulatory G protein-coupled adenylate cyclase activity in osteoblastic cells. *Am. J. Physiol.* 273, E776-E781.
- Elderstig, H., Larsson, O., 1997. Polymeric MST-high precision at low cost. *J. Micromech. Microeng.*, 7, 89-92.
- Fritton, S. P., McLeod, K. J., Rubin, C.T., 2000. Quantifying the strain history of bone: spatial uniformity and self-similarity of low-magnitude strains. *J. Biomechanics.* 33 (3), 317-325.
- Kunz, R. R., 2004. Photoresist outgassing: a potential Achilles heel for short wave-length optical lithography? in *Proc. of SPIE*, 5376, 1-15.
- Scuor, N., Gallina, P., Panchawagh, H. V., Mahajan, R. L., Sbaizero, O., 2006. Design of a novel MEMS platform for the biaxial stimulation of living cells. *Biomed. Microdevices*, 8, 239-246.
- Selvaganapathy, P., Leung Ki, Y.-S., Renaud, P., Mastrangelo, C. H., 2002. Bubble -free electrokinetic pumping. *J. Microelectromech. Syst.*, 11(5), 448-453.
- Timoshenko, S.P. and Goodier, J.N., 1970. Theory of Elasticity. 3rd ed. New York: McGraw-Hill Publishing Company. 409-415.
- U.S. Department of Health and Human Services, (2007). Bone Health and Osteoporosis: A Report of the Surgeon General. Retrieved July 9, 2007, from <http://www.surgeongeneral.gov/library/bonehealth/factsheet2.html>
- Yang, S., Saif, T., 2006. MEMS based sensors for the study of indentation response of single cells. in *Tech. Dig. of MEMS 2006*, Istanbul, Turkey, 20-23.
- You, J., Yellowley, C. E., Donahue, H. J., Jacobs, C. R., 1999. Physiological levels of substrate deformation are less stimulatory to bone cells compared to fluid flow, In *American Society of Mechanical Engineers, Bioengineering Division (Publication) BED*, 43, 161-162.
- You, L., Cowin, S. C., Schaffler, M. B., Weinbaum, S., 2001. A model for strain amplification in the actin cytoskeleton of osteocytes due to fluid drag on pericellular matrix. *J. Biomechanics.* 34 (11), 1375-1386.
- Zhang, W.-Y., 2007. Design, Modeling, Fabrication and Characterization of a MEMS Device for Measuring the Mechanical Compliance of a Biological Cell. *Ph.D. Dissertation*, Lehigh University, 2007.